J Mol Model (2013) 19:5367–5376
DOI 10.1007/s00894-013-2014-6

ORIGINAL PAPER

# A theoretical study on 1,5-diazido-3-nitrazapentane (DANP) and 1,7-diazido-2,4,6-trinitrazaheptane (DATNH): molecular and crystal structures, thermodynamic and detonation properties, and pyrolysis mechanism

**Junqing Yang · Fang Wang · Jianying Zhang · Guixiang Wang · Xuedong Gong**

Received: 21 August 2013 / Accepted: 12 September 2013 / Published online: 27 October 2013


**Abstract** 1,5-Diazido-3-nitrazapentane (DANP) and 1,7-diazido-2,4,6-trinitrazaheptane (DATNH) are two energetic plasticizers. To better understand them, a detailed theoretical investigation was carried out using density functional theory and molecular mechanics methods. The crystal structures, spectra, thermodynamic properties, heats of formation, detonation velocity, detonation pressure, specific impulse and thermal stability were estimated. Possible initiation steps of pyrolysis were discussed by considering the bond breaking of N–$NO_2$, C–$N_3$, and N–$N_2$ (via hydrogen transfer) for both compounds and the cyclization of the adjacent nitro and azido groups for DATNH. Results show that the rupture of N–$NO_2$ and N–$N_2$ (via hydrogen transfer) may happen simultaneously as the initial step of pyrolysis. Both crystals have *P*-1 symmetry as was observed experimentally. DANP has higher stability than DATNH, while DATNH has better detonation performance than DANP. In addition, DANP has a lower while DATNH has a higher specific impulse than RDX, which shows their prospects as propellant components.

**Keywords** Azido nitramine · Plasticizer · Density functional theory · Detonation performance · Pyrolysis mechanism

## Introduction

Plasticizers are important components of propellants and a significant number of studies have reported on their applications in gun and rocket propellants [1]. Energetic plasticizers can not only improve the mechanical properties but also contribute to the output energy of propellants. 1,5-diazido-3-nitrazapentane (DANP) and 1,7-diazido-2,4,6-trinitrazaheptane (DATNH) (see Fig. 1) are two energetic azido nitramine plasticizers and have been the subject of many experimental investigations [2–8]. Properties such as density, infrared (IR) spectra, and their nuclear magnetic resonance (NMR) have been investigated. The pyrolysis mechanism of DATNH has also been proposed. Oyumi [7] suggested that its thermal decomposition is initiated by the azidomethyl groups, similar to the behavior of the cyclic azido nitramine 1-(azidomethyl)-3,5,7-trinitro-1,3,5,7-tetraazacyclooctane [9], while Dang [10] supposed that the pyrolysis of DATNH comprises two stages: the first is the decomposition of N–$NO_2$ and the second is the rupture of C–$N_3$ and the remaining part of the molecule.

To clarify the pyrolysis mechanism of DATNH and to fill in the blanks in the pyrolysis mechanism of DANP, Mulliken bond populations (MBPs), natural bond orders (NBOs), and bond dissociation energies ($E_{BD}$) were calculated with density functional theory in this work. Considering that the decomposition of azido compounds may also start from the transfer of H to the N of –$N_3$ to eliminate $N_2$ [11] or to the O of –$NO_2$ to release HONO [12], or start from the cyclization of the adjacent nitro and azido groups to give off $N_2$ [13], the activation energies of the H-transfer reactions [$E_a$(H)] and the cyclization of the adjacent nitro and azido groups [$E_a$(C)] were predicted. In addition, the IR, NMR, thermodynamic functions, heats of formation, molecular packing, crystal density, detonation performance, and specific impulse values ($I_S$) were also studied. Specific impulse is a key parameter used to characterize and evaluate the properties of propellants, therefore, theoretical prediction of specific impulse makes the

J. Yang · F. Wang · J. Zhang · G. Wang · X. Gong (✉)
Department of Chemistry, Nanjing University of Science and Technology, Nanjing 210094, China
e-mail: gongxd325@mail.njust.edu.cn

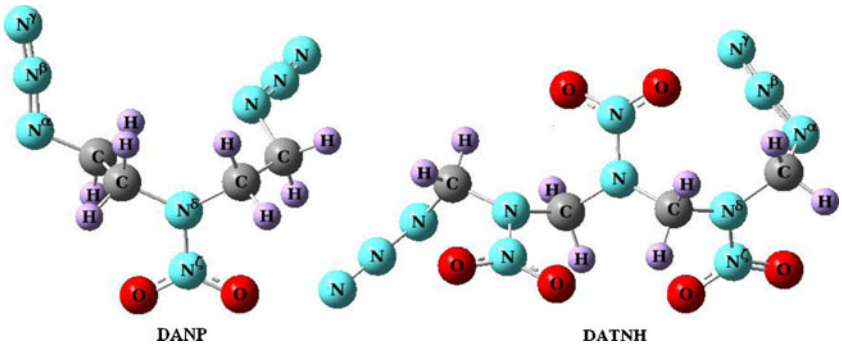


**Fig. 1** Optimized geometries of the title compounds

study more meaningful. This paper focuses on a comparison of the performance of DANP and DATNH and presents a detailed theoretical investigation on their initiation mechanism of thermolysis for the first time. This systematic theoretical work would be helpful for further studies on energetic azido nitramine compounds.

## Theoretical methods

Gaussian [14] and Materials Studio [15] program packages were employed in this study. The molecular structures were optimized using the B3LYP [16–18] method of density functional theory with the 6-31G* [19] basis set, which has been proven to be accurate enough to predict molecular structures, infrared vibration frequencies, and other properties [20–22]. The IR spectra were assigned and NMR chemical shifts were predicted at the same level. The crystal structures and densities ($\rho$) were predicted using the molecular mechanics method with the Dreiding force field [23].

Based on the vibration analysis and the statistical thermodynamic principle [24], the standard molar heat capacity ($C^0_{p,m}$), standard molar entropy ($S^0_m$), and standard molar thermal enthalpy ($H^0_m$) from 200 to 800 K were derived using the frequencies scaled by a factor 0.96 to remove the systematic overestimation [25, 26].

The gas-phase heats of formation [$\Delta H_f$(g)s] were calculated from the isodesmic reactions (1) and (2). This procedure has proved very successful and has been used widely in previous studies [27].

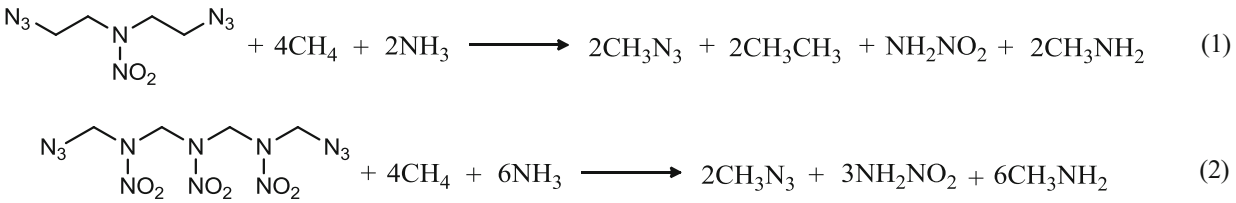


The heats of formation in solid state [$\Delta H_f$(s)s] were then estimated using the Eq. (3) [28]:

$$\Delta H_f(s) = \Delta H_f(g) - \Delta H_{sub} \quad (3)$$

where $\Delta H_{sub}$ is the sublimation enthalpy evaluated using the Eq. (4) suggested by Rice [29] and Politzer [30]:

$$\Delta H_{sub} = aA_S^2 + \beta\left(\nu\sigma^2_{tot}\right)^{0.5} + \gamma \quad (4)$$

where $A_S$ is the area of the isosurface of 0.001 e/Bohr$^3$ electron density of the molecule; $\nu$ is the degree of balance between positive and negative potential on the molecular surface; $\sigma^2_{tot}$ is a measure of variability of the electrostatic potential; $A_S$, $\nu$, and $\sigma^2_{tot}$ were calculated using a self-compiled program [31]. The values of coefficients $\alpha$ (4.234303×10$^{-4}$ kcal mol$^{-1}$ Å$^{-4}$), $\beta$ (2.5793785 kcal mol$^{-1}$), and $\gamma$ (−6.7335407 kcal mol$^{-1}$) were taken from [29].

Based on the calculated $\rho$ and $\Delta H_f$(s), detonation velocity ($D$) and detonation pressure ($P$) were predicted using the empirical Kamlet-Jacobs equations [32].

$$D = 1.01\left(N\ \overline{M}^{0.5} Q^{0.5}\right)^{0.5}(1 + 1.30\rho) \quad (5)$$

$$P = 1.558\ \rho^2 N\ \overline{M}^{0.5} Q^{0.5} \quad (6)$$

where $\rho$ is the density of the explosives (g cm$^{-3}$), $N$ is the moles of gas produced by per gram of explosives, $\overline{M}$ is the

**Table 1** Part of bond length ($r$), natural bond order (NBO) and Mulliken bond population (MBP)

| | DANP | | | DATNH | | |
|---|---|---|---|---|---|---|
| | $N^{\alpha}$- $N^{\beta}$ | $N^{\beta}$-$N^{\gamma}$ | $N^{\delta}$-$N^{\zeta}$ | $N^{\alpha}$- $N^{\beta}$ | $N^{\beta}$-$N^{\gamma}$ | $N^{\delta}$-$N^{\zeta}$ |
| $r$ /Å | 1.237 | 1.141 | 1.374 | 1.242 | 1.139 | 1.392 |
| NBO | 1.506 | 2.350 | 1.082 | 1.485 | 2.368 | 1.035 |
| MBP | 0.320 | 0.574 | 0.199 | 0.290 | 0.580 | 0.181 |

average molar weight of detonation products, and $Q$ is the chemical energy of detonation (cal $g^{-1}$). $N$, $\overline{M}$ and $Q$ were determined according to the largest exothermic principle, that is, all the N atoms turn into $N_2$, the O atoms react with the H atoms to give $H_2O$ at first, and then form $CO_2$ with the C atom. If the number of O atoms is more than that needed to oxidize H and C atoms, the redundant O atoms will convert into $O_2$. If the content of O is not enough to satisfy the full oxidation of the H and C atoms, the remaining H atoms will convert into $H_2$, and C atoms will exist as solid-state C [33]. When both C and H are redundant, they will form $CH_4$ to release more heat.

The MBPs, NBOs, the energy gaps ($E_g$s) of the frontier orbits and $E_{BD}$s were analyzed to measure the stabilities of the title compounds. The $E_{BD}$ was calculated using the following equation, as was done in previous research [34–36]:

$$E_{BD}(A{-}B) = E_{A\cdot} + E_{B\cdot} - E_{A-B} \tag{7}$$

where A–B stands for the neutral molecule and A· and B· for the corresponding radical products after the dissociation of the A–B bond; $E_{A-B}$, $E_{A\cdot}$ and $E_{B\cdot}$ are their corresponding total energies after the correction of the zero-point energy. The activation energies of reactions were calculated from the following equation:

$$E_a = E_{TS} - E_R \tag{8}$$

$E_{TS}$ and $E_R$ are the total energies after the correction of the zero-point energy for the transition state and reactant, respectively. IRC analyses were performed to verify the reliability of the transition states. Considering the important role of H atoms in the hydrogen transfer reactions, calculations of $E_{BD}$ and $E_a$(H) were also performed using the 6-31++G** basis set.

Specific impulse $I_S$ was estimated using the following equations introduced by Politzer [37] and employed by many studies [38, 39]:

$$I_s \approx T_C^{1/2} N^{1/2} \tag{9}$$

$$\Delta H_C = C_p(T_C - T_0) \tag{10}$$

$$\Delta H_C = \sum \Delta H_{f,R} - \sum \Delta H_{f,P} \tag{11}$$

where $T_0$ is the initial temperature and $T_C$ is the combustion temperature in the combustion chamber; $N$ is the number of moles of gaseous products produced by per unit weight of explosive; $\Delta H_C$ is the enthalpy of combustion; $C_p$ is the total heat capacity of the products; $\Delta H_{f,R}$ and $\Delta H_{f,P}$ are the heats of formation of the explosive and the products, respectively.

Oxygen balance ($OB$) represents the oxygen content of a compound and can be used to approximately predict the impact sensitivity of explosives [40]. It was calculated from Eq. (12):

$$OB = \left[16 \times \left(c - 2a - b/2\right)\right] \times 100/M \tag{12}$$

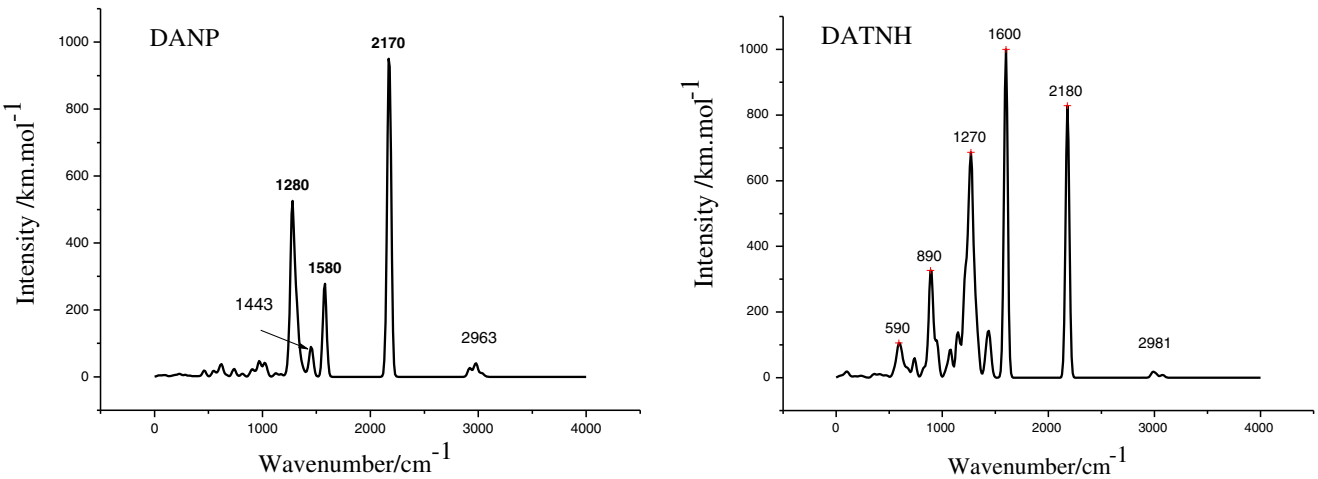


**Fig. 2** Infrared (IR) spectra calculated at the B3LYP/6-31G* level

**Table 2** Characteristic absorptions ($cm^{-1}$) in the title compounds[a]

| DANP | DATNH | Assignment |
|---|---|---|
| 2,170 (2,109 s) | 2,180 (2,130 s) | $N_3$ stretching vibration |
| 1,280 (1,275 s) | 1,270 (1,273 s) | N-$NO_2$ stretching vibration |
| 1,580 (1,519 s) | 1,600 (1,556 s) | $NO_2$ stretching vibration |
| 2,963, 1,443 (2,946 w, 1, 449 w) | 2,981 (2,980 w) | $CH_2$ stretching vibration |
| | 890 m, 590 w (890–993 m) | Skeleton vibration |

[a] Experimental values in parentheses are from [8] for DANP and [7] for DATNH; s, m and w represent strong, medium, and weak absorptions, respectively

where $M$ is the molecular weight, and $a$, $b$ and $c$ are the numbers of C, H, and O atoms, respectively, of the compound $C_aH_bO_cN_d$.

## Results and discussion

### Molecular geometrical structures

The optimized geometries of DANP and DATNH are depicted in Fig. 1. Some bond lengths, MBPs, and NBOs are listed in Table 1. The data clearly show that, for the two compounds, the $N^{\delta}$–$N^{\zeta}$ bond in the N–$NO_2$ group is longer than the $N^{\alpha}$–$N^{\beta}$ and $N^{\beta}$–$N^{\gamma}$ bonds in the azido group. $N^{\alpha}$–$N^{\beta}$ (1.237 Å in DANP and 1.242 Å in DATNH) has the obvious double-bond character and $N^{\beta}$–$N^{\gamma}$ (1.141 Å in DANP and 1.139 Å in DATNH) possesses the triple-bond character. This can also be illustrated by the value of NBOs. Taking DANP as an example, the NBOs of $N^{\alpha}$–$N^{\beta}$ and $N^{\beta}$–$N^{\gamma}$ are 1.506 and 2.350, respectively. The values (about 180.0°) of $N^{\alpha}$–$N^{\beta}$–$N^{\gamma}$ angles suggest that three N atoms of the $-N_3$ group are essentially in a straight form. In addition, it clearly shows that the bond with a longer length has smaller NBO and MBP. For example, $N^{\delta}$–$N^{\zeta}$ of N–$NO_2$ is the longest N–N bond with the smallest bond order and population.

### IR spectra

IR spectra are provided in Fig. 2 and the frequencies and the assignments of main absorptions are listed in Table 2. Because of the complexity of vibration modes, only some characteristic vibration modes were assigned in this work. The two compounds both had three main absorption bands with quite similar frequencies. The $N_3$ stretching vibration is at 2,170–2,180 $cm^{-1}$; N-$NO_2$ stretching vibration locates at 1,270–1,280 $cm^{-1}$; $NO_2$ stretching vibration is at 1,580–1,600 $cm^{-1}$. The weak peaks in the region 500–1,000 $cm^{-1}$ are caused mainly by the deformation of the molecular skeleton. As we can see from Table 2, the calculated frequencies are in accord with the experimental values. The tiny discrepancy may be due to the intermolecular interactions in the experimental sample. This proves the reliability of the simulated IR at the B3LYP/6-31G* level.

### NMR spectra

NMR spectra of the title compounds were predicted based on the geometries optimized at the B3LYP/6-31G* level. The chemical shifts of $^1H$ ($\delta_H$) and $^{13}C$ ($\delta_C$) are listed in Table 3. Here, the chemical shifts of C and H are relative to those of tetramethylsilane and the chemical shifts of N are relative to those of ammonia. It is noted that the predicted values are close to the experimental values. For DANP, the calculated $\delta_H$s are 3.543 and 4.042 ppm respectively and their corresponding experimental values are 3.636 and 3.966 ppm; the calculated $\delta_C$s are 52.472 and 47.888 ppm, respectively, and their corresponding experimental values are 51.206 and 47.994 ppm. The average relative deviation is about 1.79 %. The slight differences between the predicted and experimental data may be caused by the fact that the theoretical calculations have not taken into account the effect of the solvent. The corresponding $\delta_H$ and especially $\delta_C$ of DATNH are larger than that of DANP, obviously because of the presence of more N-$NO_2$ groups. $^{14}N$ NMR shifts ($\delta_N$s), which have not been experimentally observed, have also been predicted and shown in Fig. 3. For the two compounds, the N atoms are suited in

**Table 3** $\delta_C$ and $\delta_H$ (ppm) of the title compounds[a]

[a] Data in parentheses are experimental values from [8] for DANP and [7] for DATNH

| | $\delta_H$ (4H, $CH_2N_3$) | $\delta_H$ (4H, $CH_2N$) | $\delta_C$ (2C, $CH_2N_3$) | $\delta_C$ (2C, $CH_2N$) |
|---|---|---|---|---|
| DANP | 3.543(3.636) | 4.042(3.966) | 52.472(51.206) | 47.888(47.994) |
| DATNTH | 4.126(4.5) | 4.863(5.0) | 64.971 | 62.787 |

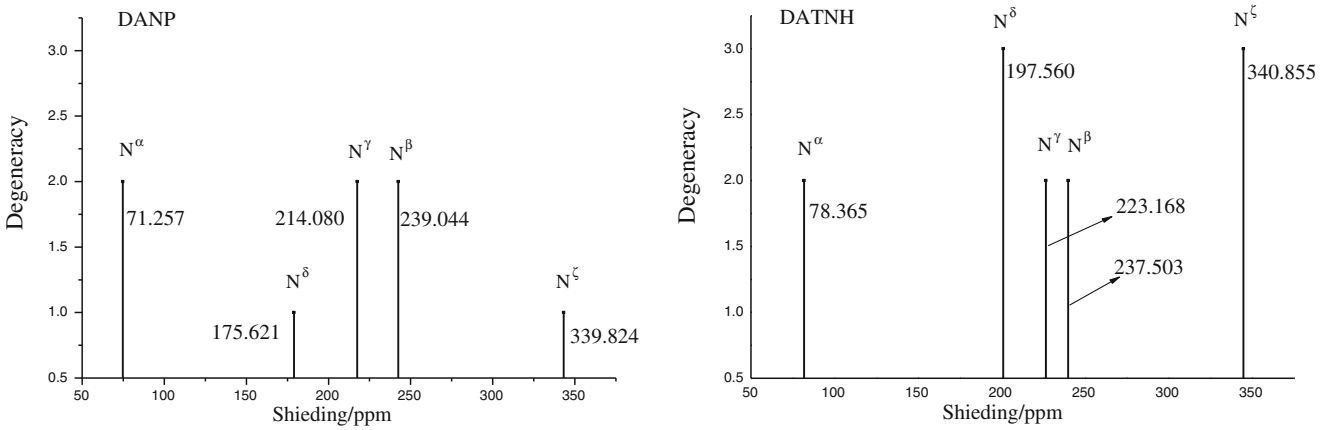


**Fig. 3** $^{14}$N NMR spectra calculated at the B3LYP/6-31G* level

five chemical environments and the order of $\delta_N$ is $N^\zeta > N^\beta > N^\gamma > N^\delta > N^\alpha$. The calculated $\delta_N$s of $N^\alpha$, $N^\beta$, and $N^\gamma$ are 71.257, 239.044, and 214.080 ppm in DANP, respectively, and the corresponding data in DATNH are 78.365, 237.503, and 223.168 ppm. This suggests that the number of the N–$NO_2$ group affects the chemical shifts of N atoms, especially $N^\alpha$ and $N^\gamma$ in the $-N_3$ group.

## Thermodynamic properties

Thermodynamic properties of the two compounds were evaluated and tabulated in Table 4. It can be seen that $C^0_{p,m}$, $S^0_m$, and $H^0_m$ increase evidently with the increasing temperature from 200 to 800 K. This is because, at the higher temperature, the vibrations of molecules are intensified and make more contributions to the thermodynamic properties, but at the lower temperature the main contributions are from translation and rotation. Therefore, the increase in temperature leads to the increase of thermodynamic functions. In addition, all the thermodynamic properties of DATNH are larger than those of DANP at the same temperature for the bigger and more complex structure.

The relationships between thermodynamic functions and temperature are shown as follows and in Fig. 4. Obviously, the increments for $C^0_{p,m}$ and $S^0_m$ decrease with the increasing temperature, while that for $H^0_m$ increases. The corresponding correlation coefficients are all 0.9999. These equations will be helpful for further studies on the other physical, chemical, and explosive properties of the title compounds at various temperatures.

DANP
$$C^0_{p,m} = 57.0360 + 1.0186T - 4.9739 \times 10^{-4}T^2$$
$$S^0_m = 334.8263 + 1.2892T - 3.9258 \times 10^{-4}T^2$$
$$H^0_m = -14.8191 + 0.1714T + 2.5958 \times 10^{-4}T^2$$

DATNH
$$C^0_{p,m} = 38.7862 + 0.6761T - 3.0300 \times 10^{-4}T^2$$
$$S^0_m = 297.7260 + 0.8582T - 2.47481 \times 10^{-4}T^2$$
$$H^0_m = -8.0497 + 0.1077T + 1.8673 \times 10^{-4}T^2$$

## Molecular packing

Table 5 collects the cell parameters of the seven possible packings with the lowest energy in each of seven space groups. We see that the structures with the $P$-1 symmetry have the lowest energy for both compounds. This means they most probably belong to the $P$-1 space group (Fig. 5), since the stable polymorph usually possesses lower Gibbs free energy (or total energy at 0 K). The predicted cell parameters and crystal density of DATNH with the $P$-1 symmetry ($a$ = 6.95 Å, $b$ = 10.23 Å, $c$ = 10.91 Å, $\alpha$ = 111.98°, $\beta$ = 107.89°, $\gamma$ = 92.27°, $Z$ = 2, $\rho$ = 1.70 g cm$^{-3}$) are close to the corresponding

**Table 4** Thermodynamic properties of DANP and DATNH at different temperatures

| | $T$/K | 200 | 300 | 400 | 500 | 600 | 700 | 800 |
|---|---|---|---|---|---|---|---|---|
| DANP | $C^0_{p,m}$/(J mol$^{-1}$ K$^{-1}$) | 162.97 | 213.31 | 261.06 | 302.01 | 335.64 | 363.12 | 385.77 |
| | $S^0_m$/(J mol$^{-1}$ K$^{-1}$) | 458.23 | 533.81 | 601.84 | 664.63 | 722.77 | 776.64 | 826.65 |
| | $H^0_m$/(kJ mol$^{-1}$) | 21.78 | 40.59 | 64.35 | 92.57 | 124.51 | 159.49 | 196.97 |
| DATNH | $C^0_{p,m}$/(J mol$^{-1}$ K$^{-1}$) | 241.09 | 317.27 | 385.94 | 442.93 | 488.59 | 525.04 | 554.42 |
| | $S^0_m$/(J mol$^{-1}$ K$^{-1}$) | 575.2 | 687.48 | 788.41 | 880.88 | 965.82 | 1,043.98 | 1,116.07 |
| | $H^0_m$/(kJ mol$^{-1}$) | 31.19 | 59.14 | 94.39 | 135.93 | 182.6 | 233.35 | 287.37 |

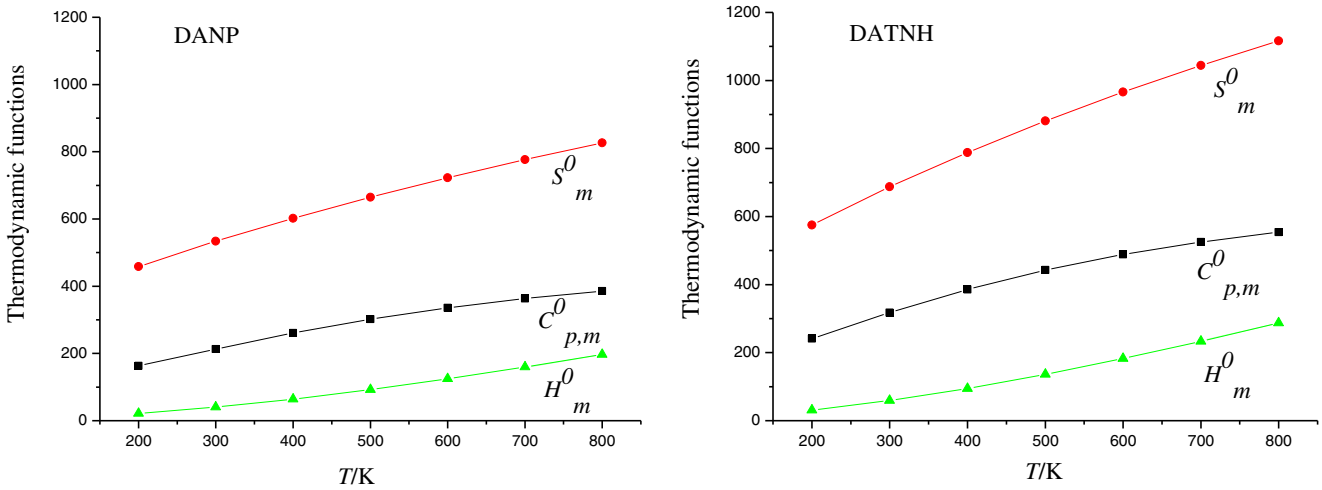


**Fig. 4** Relationships between $C^0_{p,m}$(J mol$^{-1}$ K$^{-1}$), $S^0_m$(J mol$^{-1}$ K$^{-1}$), $H^0_m$(kJ mol$^{-1}$) and $T$(K)

experimental values ($a$=6.407 Å, $b$=9.793 Å, $c$=10.801 Å, $\alpha$=109.52°, $\beta$=102.19°, $\gamma$=94.91°, $Z$=2, $\rho$=1.72 g cm$^{-3}$) [7], which indicates the Dreiding force field is reliable for predicting the crystal structure of DATNH. Actually, it has been used widely in predicting molecular crystals and the results proved quite reliable [41, 42]. Therefore, we believe the predicted cell parameters of DANP ($a$=4.77 Å, $b$=9.97 Å, $c$=17.33 Å, $\alpha$=51.51°, $\beta$=50.51°, $\gamma$=51.88°, $Z$=2, $\rho$=1.43 g cm$^{-3}$) are also reasonable. DANP has a much lower density than DATNH, which may imply it has lower detonation velocity and pressure than DATNH since density is a critical factor of detonation performance.

## Pyrolysis mechanism and stability

Table 6 collects the energies of the highest occupied molecular orbital ($E_{HOMO}$) and the lowest unoccupied molecular orbital ($E_{LUMO}$) and their energy gap ($E_g$). The $E_g$ of the frontier orbits can be used to evaluate the chemical stability of the compounds with similar structures. It has been proposed that

**Table 5** Cell parameters predicted with the Dreiding force field

| | Parameters | $C2/c$ | $P2_1$ | $P2_1/C$ | $P$-1 | $P2_12_12_1$ | $Pbac$ | $Pna2_1$ |
|---|---|---|---|---|---|---|---|---|
| DANP | $Z$ | 8 | 2 | 4 | 2 | 4 | 8 | 4 |
| | $\rho$(g cm$^{-3}$) | 1.40 | 1.39 | 1.41 | 1.43 | 1.39 | 1.41 | 1.36 |
| | $E$(kcal mol$^{-1}$ cell$^{-1}$) | 3.66 | 4.11 | 3.78 | 3.22 | 4.17 | 3.76 | 4.72 |
| | $a$(Å) | 23.13 | 10.63 | 11.61 | 4.77 | 7.36 | 12.14 | 6.25 |
| | $b$(Å) | 6.21 | 7.64 | 24.21 | 9.97 | 11.82 | 21.63 | 19.12 |
| | $c$(Å) | 19.21 | 5.90 | 7.44 | 17.33 | 10.98 | 7.18 | 8.17 |
| | $\alpha$ (º) | 90 | 90 | 90 | 51.51 | 90 | 90 | 90 |
| | $\beta$ (º) | 136.53 | 92.78 | 153.25 | 50.51 | 90 | 90 | 90 |
| | $\gamma$ (º) | 90 | 90 | 90 | 51.88 | 90 | 90 | 90 |
| DATNH | $Z$ | 8 | 2 | 4 | 2 | 4 | 8 | 4 |
| | $\rho$(g cm$^{-3}$) | 1.60 | 1.61 | 1.63 | 1.70 | 1.59 | 1.57 | 1.59 |
| | $E$(kcal mol$^{-1}$ cell$^{-1}$) | 19.23 | 18.89 | 18.35 | 18.20 | 19.34 | 18.76 | 19.87 |
| | $a$(Å) | 16.27 | 6.56 | 7.05 | 6.95 | 18.46 | 22.92 | 12.19 |
| | $b$(Å) | 6.68 | 16.84 | 33.46 | 10.23 | 10.77 | 12.88 | 9.41 |
| | $c$(Å) | 30.30 | 7.07 | 6.59 | 10.91 | 6.73 | 9.19 | 11.69 |
| | $\alpha$ (º) | 90 | 90 | 90 | 111.98 | 90 | 90 | 90 |
| | $\beta$ (º) | 54.01 | 122.30 | 122.86 | 107.89 | 90 | 90 | 90 |
| | $\gamma$ (º) | 90 | 90 | 90 | 94.91 | 90 | 90 | 90 |

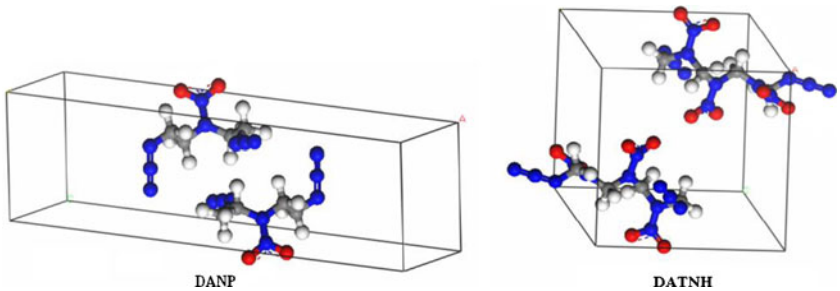


**Fig. 5** Most likely packings for DANP and DATNH

the molecule with a larger $E_g$ is expected to have a higher stability [43, 44]. According to the calculated results, the $E_g$s of the two compounds are close and the difference is about 14 kJ/mol. This suggests that their stabilities will be comparable in the chemical or photochemical process with electron transfer or leap.

The bond dissociation energy is often used to investigate the thermal stability and pyrolysis mechanism of energetic compounds. Generally, the bond that requires the minimum energy to break is the weakest bond and is most likely to be the trigger bond. To elucidate the pyrolysis mechanism of the title compounds, ruptures of N–$NO_2$, C–$N_3$ and N–$N_2$ were considered. The pyrolysis pathways of the $N_2$ elimination through the transfer of H and the cyclization of the adjacent nitro and azido groups were also considered (Fig. 6). The results showed that the breaking of N–$N_2$ is completed through the transfer of H simultaneously.

Table 7 shows the energies required for all possible initial steps of the pyrolysis. DATNH has three N-$NO_2$, the bond dissociation energies of N–$NO_2$ [$E_{BD}$(N–$NO_2$)] on the two sides are similar to each other (about 157.56 kJ $mol^{-1}$) and lower than that of the middle one (170.89 kJ $mol^{-1}$). The $E_{BD}$(N–$NO_2$) in Table 7 refers to that of the side N–$NO_2$.

According to the calculated results in Table 7, $E_{BD}$(N–$NO_2$)s are very close to the activation energies of the $N_2$ elimination process through the transfer of H [$E_a$(H)], especially at the B3YP/6-31++G** level. The $E_{BD}$(N-$NO_2$) and $E_a$(H) of DANP are 155.84 and 156.59 kJ $mol^{-1}$, respectively, and corresponding results of DATNH are 144.54 and 146.32 kJ $mol^{-1}$. $E_{BD}$(N–$NO_2$) and $E_a$(H) are much lower than the $E_{BD}$ of C–$N_3$ (267.56 kJ $mol^{-1}$ for DANP and 216.51 kJ $mol^{-1}$ for DATNH). They are also much lower than the activation energy of the cyclization reaction [$E_a$(C)] of the adjacent nitro and azido groups for DATNH. This means that reactions (13) and (14) happen much more easily than (15).

**Table 6** Energies (a.u.) of the frontier orbits and their gap

| | $E_{HOMO}$ | $E_{LUMO}$ | $E_g$ |
|---|---|---|---|
| DANP | −0.26058 | −0.05736 | 0.20322 |
| DATNH | −0.28111 | −0.08332 | 0.19779 |

Therefore, the rupture of N–$NO_2$ to give off $NO_2$ and the breaking of N–$N_2$ via the H transfer to release $N_2$ may happen at almost the same time as the initial pyrolysis step. The breaking of C–$N_3$ and the cyclization of adjacent nitro and azido groups cannot be the initial step of the pyrolysis of DANP and DATNH. This conclusion is different from that suggested in references [7] and [10]. It is also worth noting that the H transfer reactions of DANP and DATNH are both exothermic and the enthalpies of reactions are −176.35 and −185.24 kJ $mol^{-1}$ respectively, while the rupture of N-$NO_2$ is endothermic. Compared with $CH_3N_3$ ($E_a$(H)= 156.30 kJ $mol^{-1}$[11]), the calculated $E_a$(H) of DANP is essentially the same and that of DATNH is about 10 kJ $mol^{-1}$ lower, which shows DANP has a stability comparable with that of $CH_3N_3$, while DATNH has a lower stability than $CH_3N_3$. Comparing the $E_{BD}$ of N–$NO_2$ of the title compounds with that of RDX (175.77 kJ $mol^{-1}$ at the B3LYP/6-31G* level) [45], the N–$NO_2$ bonds in DANP and DATNH, especially the latter, have lower strengths, which suggests the title compounds have lower stability than RDX. However, they both satisfy the requirement of the stability for energetic compounds ($E_{BD}$≈80–120 kJ $mol^{-1}$ [46]) and DANP is somewhat more stable than DATNH.

## Heats of formation and detonation properties

Table 8 summarizes the $\Delta H_f$(g), $\Delta H_{sub}$, and $\Delta H_f$(s) of the title compounds and the related parameters of $A_S$, $\sigma^2_{tot}$, and $\nu$. In comparison with the available experimental $\Delta H_f$(s) of DATNH (617.23 kJ $mol^{-1}$[47]), the calculated value (598.74 kJ $mol^{-1}$) gives a reasonable agreement with a relative error 3.00 %. This suggests the reliability of the calculation methods and the results for the similar molecule DANP.

Table 9 collects the predicted densities, detonation velocity, detonation pressure, oxygen balance and specific impulse for DANP and DATNH. For comparison, the detonation performance (both the calculated and experimental data) of RDX is also listed.

The detonation properties of DATNH are better than those of DANP since DATNH has much bigger $\rho$ and $Q$. $D$ and $P$ of DATNH are 8.38 km $s^{-1}$ and 30.06 GPa, respectively. Corresponding values for DANP are 7.03 km $s^{-1}$ and 18.91 GPa. The relative specific impulses $I_{S,r}$ of DANP and

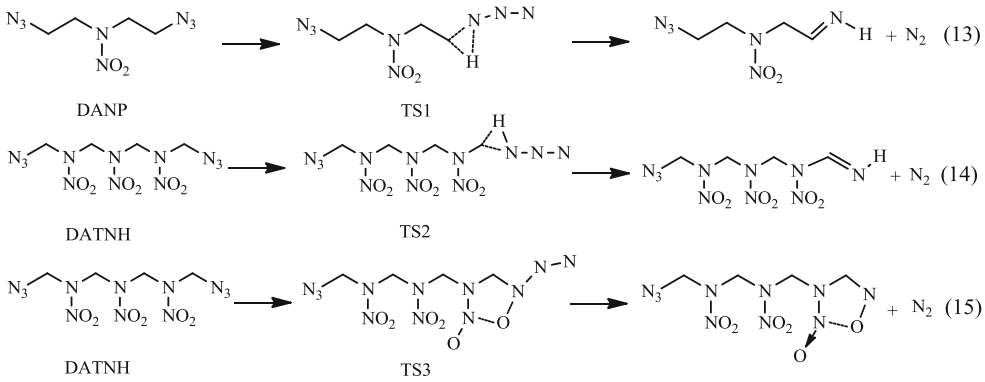


**Fig. 6** $N_2$ elimination process through H-transfer and cyclization

**Table 7** Bond dissociation energy ($E_{BD}$) and activation energy ($E_a$) [a]

| | $E_{BD}$(N-$NO_2$)/(kJ mol$^{-1}$) | $E_{BD}$(C-$N_3$)/(kJ mol$^{-1}$) | $E_a$(H)/(kJ mol$^{-1}$) | $E_a$(C)/(kJ mol$^{-1}$) |
|---|---|---|---|---|
| DANP | 173.43 (155.84) | 274.66 (267.56) | 165.70 (156.59) | |
| DATNH | 157.56 (144.54) | 228.16 (216.51) | 154.83 (146.32) | 193.11 |

[a] $E_a$(H) and $E_a$(C) are the activation energies of the H transfer reaction and cyclization reaction, respectively. Data in parentheses are calculated at the B3LYP/6-31++G** level.

**Table 8** Calculated heats of formation and related parameters

| | $A_S$/(Å$^2$) | $\sigma^2_{tot}$ | $\nu$ | $\Delta H_f$(g)/(kJ mol$^{-1}$) | $\Delta H_{sub}$/(kJ mol$^{-1}$) | $\Delta H_f$(s)/(kJ mol$^{-1}$) |
|---|---|---|---|---|---|---|
| DANP | 224.42 | 129.91 | 0.25 | 610.87 | 122.06 | 488.81 |
| DATNH | 292.97 | 139.46 | 0.19 | 778.56 | 179.82 | 598.74 (617.23 [47]) |

**Table 9** Detonation properties of DANP, DATNH, and RDX[a]

| | DANP | DATNH | RDX |
|---|---|---|---|
| $\rho$/(g cm$^{-3}$) | 1.43 | 1.70 | 1.80 (1.82) |
| $Q$/(cal g$^{-1}$) | 1,161.21 | 1,462.75 | 1,632.76 |
| $D$/(km s$^{-1}$) | 7.03 | 8.38 | 8.93 (8.75) |
| $P$/GPa | 18.91 | 30.06 | 35.36 (34.00) |
| $I_S$/s | 195.97 | 248.27 | 212.98 |
| $I_{S,r}$ | 0.92 | 1.16 | 1.00 |
| $OB$/% | −79.90 | −29.98 | −21.61 (−21.61) |

[a] Values in parentheses are experimental data from [48].

DATNH to RDX are 0.92 and 1.16, which means DANP has a somewhat lower while DATNH has a higher $I_S$ than RDX. This makes the title compounds, especially DATNH, good candidates for propellant components. Though their detonation velocity and detonation pressure are not very high, as the plasticizers, they can improve the specific impulse, while not significantly lowering the output energy of the propellant.

The agreement of the predicted $\rho$, $D$, and $P$ (1.80 g cm$^{-3}$, 8.93 km s$^{-1}$ and 35.36 GPa, respectively) with the corresponding experimental results (1.82 g cm$^{-3}$, 8.75 km s$^{-1}$ and 34.00 GPa, respectively [48]) for RDX again shows the reliability of the calculation results of this study.

## Conclusions

In this study, systematic calculations were performed on two azido nitramine plasticizers, DANP and DATNH, with density functional theory and molecular mechanics methods. The consistence between the theoretical and experimental results verifies the reliability of this work. Thermolysis of the title compounds may be initiated simultaneously from $N_2$ elimination (N–$N_2$ breaking) through H transfer and the rupture of N–$NO_2$. DANP has higher stability, while DATNH has better detonation properties. Compared with RDX, DATNH has a higher and DANP has a somewhat lower specific impulse. Though both of them have smaller detonation velocity and detonation pressure than RDX, it will not limit their

applications since they act mainly as plasticizers in composite explosives and propellants. Their high specific impulses make them good components of propellants. This paper provides some basic information for people interested in these and similar compounds.

**Acknowledgments** We gratefully thank the Research Fund for the Doctoral Program of Higher Education of China (NO.20103219120014), Natural Science Foundation of Jiangsu Province (NO. BK20130755), and NUST "Excellent Plan and Zijin Star" Research Foundation for their support of this work.

## Reference

1. Provatas A (2000) Energetic polymers and plasticisers for explosive formulations—a review of recent advances. DSTO-TR-0966.
2. Flanagan JE, Wilson ER, Frankel MB (1991) 1, 5-diazido-3-nitrazapentane and method of preparation thereof. US: 5013856
3. Ji YP, Lan Y, Li PR, Wang W, Ding F, Liu YJ (2008) Synthesis and characterization of 1,5-diazido-3-nitrazapentane (DIANP). Chin J Explos Propell 31:44–46
4. Zhang ZZ, Wang BZ, Shi ZC, Ji YP, Liu Q, Zhu CH (2003) Synthesis and properties of 1,7-Diazido-2,4, 6-trinitro-2,4,6-triazoheptane. Chin J Explos Propell 26:3–5
5. Klapötke TM, Krumm B, Steemann FX (2009) Preparation, characterization, and sensitivity data of some azidomethyl nitramines. Propell Explos Pyrotech 34:13–23
6. Wang JL, Ji YP, Gao FL, Guo W, Ren ST (2011) Experimental measurement of safety parameters of DIANP. Chin J Energ Mater 19:693–696
7. Oyumi Y, Rheingold A, Brill T (1987) Thermal decomposition of energetic materials. 19. Unusual condensed-phase and thermolysis properties of a mixed azidomethyl nitramine: 1,7-diazido-2,4,6-trinitro-2,4,6-triazaheptane. J Phys Chem 91:920–925
8. Wang W, Ding F, Liang Y, Ji YP, Liu WX (2010) Preparation and characterization of DIANP certified reference material. Chin J Explos Propell 33:52–55
9. Brill T, Karpowicz R, Haller T, Rheingold A (1984) A structural and fourier-transform infrared-spectroscopic characterization of the thermal decomposition of 1-(azidomethyl)-3,5,7-trinitro-1,3,5,7-tetraazacyclooctane. J Phys Chem 88:4138–4143
10. Dang ZM, Zhao FQ (2000) Thermal decomposition characteristics of low signature propellant containing 1,7-diazido-2,4,6-trinitrazaptane. Xi'an JiaoTong University XueBao 34:88–92
11. Quinto-Hernandez A, Wodtke AM, Bennett CJ, Kim YS, Kaiser RI (2010) On the interaction of methyl azide ($CH_3N_3$) ices with ionizing radiation: formation of methanimine ($CH_2NH$), hydrogen cyanide (HCN), and hydrogen isocyanide (HNC). J Phys Chem A 115:250–264
12. Chakraborty D, Muller RP, Dasgupta S, Goddard WA (2000) The mechanism for unimolecular decomposition of RDX (1,3,5-trinitro-1,3,5-triazine), an ab initio study. J Phys Chem A 104:2261–2272
13. Li JS, Xiao HM, Gong XD, Dong HS (1999) Theoretical study on the mechanism, thermodynamics and kinetics of 2-azido-1,3,5-trinitrobenzene thermolysis. Explos Shock Waves 19:1–5
14. Frisch MJ, Trucks GW, Schlegel HB, Suzerain GE, Robb MA, Cheeseman JrJR, Montgomery JA, Vreven T, Kudin KN, Burant JC, Millam JM, Iyengar SS, Tomasi J, Barone V, Mennucci B, Cossi M, Scalmani G, Rega N, Petersson GA, Nakatsuji H, Hada M, Ehara M, Toyota K, Fukuda R, Hasegawa J, Ishida M, Nakajima T, Honda Y, Kitao O, Nakai H, Klene M, Li X, Knox JE, Hratchian HP, Cross JB, Bakken V, Adamo C, Jaramillo J, Gomperts R, Stratmann RE, Yazyev O, Austin AJ, Cammi R, Pomelli C, Ochterski JW, Ayala PY, Morokuma K, Voth GA, Salvador P, Dannenberg JJ, Zakrzewski VG, Dapprich S, Daniels AD, Strain MC, Farkas O, Malick DK, Rabuck AD, Raghavachari K, Foresman JB, Ortiz JV, Cui Q, Baboul AG, Clifford S, Cioslowski J, Stefanov B, Liu G, Liashenko A, Piskorz P, Komaromi I, Martin RL, Fox DJ, Keith T, Al-Laham MA, Peng CY, Nanayakkara A, Challacombe M, Gill PMW, Johnson B, Chen W, Wong MW, Gonzalez C, Pople JA (2004) Gaussian 03, Revision B.05, Gaussian: Wallingford.
15. Materials Studio 4.4 (2008) Accelrys, San Diego, CA
16. Lee C, Yang W, Parr RG (1988) Development of the Colle-Salvetti correlation-energy formula into a functional of the electron density. Phys Rev B 37:785–789
17. Becke AD (1992) Density-functional thermochemistry. II. The effect of the Perdew–Wang generalized-gradient correlation correction. J Chem Phys 97:9173–9177
18. Becke AD (1993) Density-functional thermochemistry. III. The role of exact exchange. J Chem Phys 98:5648–5652
19. Hariharan PC, Pople JA (1973) The influence of polarization functions on molecular orbital hydrogenation energies. Theor Chim Acta 28:213–222
20. Xu XJ, Xiao HM, Gong XD, Ju XH, Chen ZX (2005) Theoretical studies on the vibrational spectra, thermodynamic properties, detonation properties, and pyrolysis mechanisms for polynitroadamantanes. J Phys Chem A 109:11268–11274
21. Gong XD, Xiao HM (2001) Studies on the molecular structures, vibrational spectra and thermodynamic properties of organic nitrates using density functional theory and ab initio methods. J Mol Struct THEOCHEM 572:213–221
22. Qiu L, Xiao HM, Ju XH, Gong XD (2005) Theoretical study of the structures and properties of cyclic nitramines: tetranitrotetraazadecalin (TNAD) and its isomers. Int J Quantum Chem 105:48–56
23. Mayo SL, Olafson BD, Goddard WA (1990) Dreiding: a generic force field for molecular simulations. J Phys Chem 94:8897–8909
24. Hill TL (1960) An introduction to statistical thermodynamics. Courier Dover, New York
25. Scott AP, Radom L (1996) Harmonic vibrational frequencies: an evaluation of Hartree-Fock, Møller-Plesset, quadratic configuration interaction, density functional theory, and semiempirical scale factors. J Phys Chem 100:16502–16513
26. Wong MW (1996) Vibrational frequency prediction using density functional theory. Chem Phys Letters 256:391–399
27. Haynes WM, Lide DR, Bruno TJ (2012) CRC handbook of chemistry and physics. Taylor and Francis (CRC), Boca Raton
28. Atkins PW, Clugston MJ (1982) Principles of physical chemistry. Oxford University Press, Oxford
29. Rice BM, Pai SV, Hare J (1999) Predicting heats of formation of energetic materials using quantum mechanical calculations. Combust Flame 118:445–458
30. Politzer P, Ma Y, Lane P, Concha MC (2005) Computational prediction of standard gas, liquid, and solid-phase heats of formation and heats of vaporization and sublimation. Int J Quantum Chem 105:341–347
31. Gong XD (2007) Potden v.2.0. Nanjing University of Science and Technology: Nanjing.
32. Kamlet MJ, Jacobs SJ (1968) Chemistry of detonations. I. A simple method for calculating detonation properties of C-H-N-O explosives. J Chem Phys 48:23–35
33. Politzer P, Murray JS (2011) Some perspectives on estimating detonation properties of C, H, N, O compounds. Central Eur J Energ Mater 8:209–220
34. Wang GX, Gong XD, Xiao HM (2009) Theoretical investigation on density, detonation properties, and pyrolysis mechanism of nitro derivatives of benzene and aminobenzenes. Int J Quantum Chem 109:1522–1530
35. Zhang JY, Du HC, Wang F, Gong XD, Huang YS (2011) DFT studies on a high energy density cage compound 4-trinitroethyl-2, 6, 8, 10,

12-pentanitrohezaazaisowurtzitane. J Phys Chem A 115:6617–6621
36. Wang F, Du HC, Zhang JY, Gong XD (2011) Computational studies on the crystal structure, thermodynamic properties, detonation performance, and pyrolysis mechanism of 2,4,6,8-tetranitro-1,3,5,7-tetraazacubane as a novel high energy density material. J Phys Chem A 115:11788–11795
37. Politzer P, Murray J, Grice M, Sjoberg P, Olah G, Squire D (1991) Chemistry of energetic materials. Academic, San Diego
38. Wang GX, Gong XD, Liu Y, Du HC, Xu XJ, Xiao HM (2011) Looking for high energy density compounds applicable for propellant among the derivatives of DPO with $-N_3$, $-ONO_2$, and $-NNO_2$ groups. J Comput Chem 32:943–952
39. Wang GX, Gong XD, Du HC, Liu Y, Xiao HM (2011) Theoretical prediction of properties of aliphatic polynitrates. J Phys Chem A 115: 795–804
40. Kamlet M, Adolph H (1979) The relationship of impact sensitivity with structure of organic high explosives. II. Polynitroaromatic explosives. Propell Explos Pyrotech 4:30–34
41. Xu XJ, Zhu WH, Xiao HM (2008) Molecular packing prediction and periodic calculations on three polynitroadamantanes as potential high energy density compounds. Chin J Chem 26:602–606
42. Ghule V, Jadhav P, Patil R, Radhakrishnan S, Soman T (2009) Quantum-chemical studies on hexaazaisowurtzitanes. J Phys Chem A 114:498–503
43. Li YF, Fan XW, Wang ZY, Ju XH (2009) A density functional study of substituted pyrazole derivatives. J Mol Struct: THEOCHEM 896: 96–102
44. Ju XH, Wang ZY, Yan XF, Xiao HM (2007) Density functional theory studies on dioxygen difluoride and other fluorine/oxygen binary compounds: availability and shortcoming. J Mol Struct: THEOCHEM 804:95–100
45. Harris NJ, Lammertsma K (1997) Ab initio density functional computations of conformations and bond dissociation energies for hexahydro-1, 3, 5-trinitro-1, 3, 5-triazine. J Am Chem Soc 119:6583–6589
46. Xiao HM, Xu XJ, Qiu L (2008) Theoretical design of high energy density materials. Science, Beijing
47. Flanagan JE, Grant LE, Thompson WW, Woolery D (1985) The stable pyrolysis products of the monomers. Air Force Rocket Propulsion Laboratory, Junction , CA
48. Talawar M, Sivabalan R, Mukundan T, Muthurajan H, Sikder A, Gandhe B, Rao AS (2009) Environmentally compatible next generation green energetic materials (GEMs). J Hazard Mater 161:589–607